Chapter 3
Dissipation, Noise and Adaptive Systems

Dynamical systems are generically not isolated but interact with the embedding environment and one speaks of noise whenever the impact of the dynamics of the environment cannot be predicted. The dynamical flow slows down when energy is dissipated to the environment, approaching attracting states which may be regular, such as fixpoints or limit cycle, or irregular, such as chaotic attractors. Adaptive systems alternate between phases when they dissipate energy and times when energy is taken up form the environment, with the steady state being characterized by a balance between these two opposing processes.

In this chapter an introduction to adaptive, dissipative and stochastic systems will be given together with important examples from the real of noise controlled dynamics, like diffusion, random walks and stochastic escape and resonance.

3.1 Dissipation and Adaption

In Chap. **??** we discussed deterministic dynamical systems, viz systems for which the time evolution can be computed exactly, at least in principle, once the initial conditions are known. We now turn to "stochastic systems", i.e. dynamical systems that are influenced by noise and fluctuations. When only the mean impact of the noise is taken into account one speaks of "dissipation".

3.1.1 Dissipative Systems and Phase Space Contraction

Friction and Dissipation Friction plays an important role in real-world systems. One speaks also of "dissipation" since energy is dissipated away by friction in physical systems.

The total energy, however, is conserved in nature and friction then just stands for a transfer process of energy; when energy is transferred from a system we observe, like a car on a motorway with the engine turned off, to a system not under observation, such as the surrounding air. In this case the combined kinetic energy of the car and the thermal energy of the air body is constant; the air heats up a little bit while the car slows down.

The Mathematical Pendulum As an example we consider the damped *mathematical pendulum*

$$\ddot{\phi} + \gamma\,\dot{\phi} + \omega_0^2\,\sin\phi = 0\ , \tag{3.1}$$

which describes a pendulum with a rigid bar, capable of turning over completely, with ϕ corresponding to the angle between the bar and the vertical. The mathematical pendulum reduces to the damped harmonic oscillator for small $\phi \approx \sin\phi$, which is damped/critical/overdamped for $\gamma < 2\omega_0$, $\gamma = 2\omega_0$ and $\gamma > 2\omega_0$.

In the absence of damping, $\gamma = 0$, the energy

$$E = \frac{\dot{\phi}^2}{2} - \omega_0^2 \cos\phi \tag{3.2}$$

is conserved:

$$\frac{d}{dt}E = \dot{\phi}\,\ddot{\phi} + \omega_0^2\dot{\phi}\sin\phi = \dot{\phi}\left(\ddot{\phi} + \omega_0^2\sin\phi\right) = -\gamma\dot{\phi}^2\ ,$$

with the help of (3.1).

Normal Coordinates Transforming the damped mathematical pendulum Eq. (3.1) to a set of coupled first-order differential equations via $x = \phi$ and $\dot{\phi} = y$ one gets

$$\begin{aligned} \dot{x} &= y \\ \dot{y} &= -\gamma y - \omega_0^2 \sin x\ . \end{aligned} \tag{3.3}$$

The phase space is $\boldsymbol{x} \in \mathbb{R}^2$, with $\boldsymbol{x} = (x, y)$. For all $\gamma > 0$ the motion approaches one of the equivalent global fixpoints $(2\pi n, 0)$ for $t \to \infty$ and $n \in$ Z.

Phase Space Contraction Near an attractor the phase space contracts. We consider a three-dimensional phase space (x, y, z) for illustrational purposes. The quantity

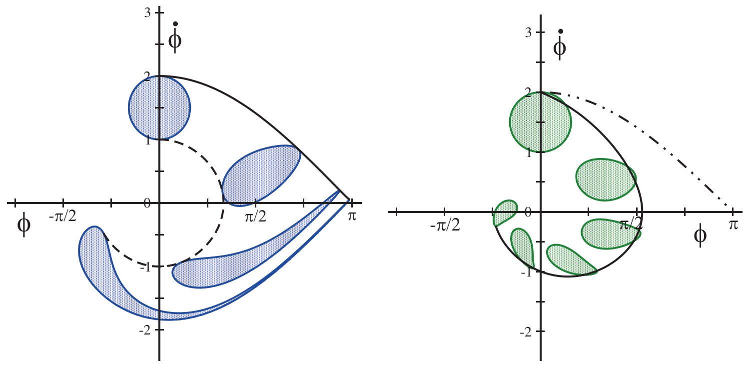

Fig. 3.1 Simulation of the mathematical pendulum $\ddot{\phi} = -\sin(\phi) - \gamma\dot{\phi}$. The *shaded regions* illustrate the evolution of the phase space volume for consecutive times, starting with $t = 0$ (*top*). *Left*: Dissipationless case $\gamma = 0$. The energy, see Eq. (3.2), is conserved as well as the phase space volume (Liouville's theorem). The *solid/dashed lines* are the trajectories for $E = 1$ and $E = -0.5$, respectively. *Right*: Case $\gamma = 0.4$. Note the contraction of the phase space volume

$$\Delta V(t) = \Delta x(t)\Delta y(t)\Delta z(t) = (x(t) - x'(t))\,(y(t) - y'(t))\,(z(t) - z'(t))$$

corresponds to a small volume of phase space. Its time evolution is given by

$$\frac{\mathrm{d}}{\mathrm{d}t}\Delta V = \Delta\dot{x}\Delta y\Delta z + \Delta x\Delta\dot{y}\Delta z + \Delta x\Delta y\Delta\dot{z}\ ,$$

or

$$\frac{\Delta\dot{V}}{\Delta x\Delta y\Delta z} = \frac{\Delta\dot{x}}{\Delta x} + \frac{\Delta\dot{y}}{\Delta y} + \frac{\Delta\dot{z}}{\Delta z} = \vec{\nabla}\cdot\dot{\boldsymbol{x}}\ , \tag{3.4}$$

where the right-hand side corresponds to the trace of the Jacobian. In Fig. 3.1 the time evolution of a phase space volume is illustrated for the case of the mathematical pendulum. An initially simply connected volume of the phase space thus remains under the effect of time evolution, but may undergo substantial
deformations.

Dissipative and Conserving Systems. A dynamical system is dissipative, if its phase space volume contracts continuously, $\vec{\nabla}\cdot\dot{\boldsymbol{x}} < 0$, for all $\boldsymbol{x}(t)$. The system is said to be conserving if the phase space volume is a constant of motion, viz if $\boldsymbol{\nabla}\cdot\dot{\boldsymbol{x}} \equiv 0$.

Mechanical systems, i.e. systems described by Hamiltonian mechanics, are all conserving in the above sense. One denotes this result from classical mechanics as "Liouville's theorem".

Mechanical systems in general have bounded and non-bounded orbits, depending on the energy. The planets run through bounded orbits around the sun, to give an example, but some comets leave the solar system for ever on unbounded trajectories. One can easily deduce from Liouville's theorem, i.e. from phase space conservation, that bounded orbits are ergodic. They come arbitrarily close to every point in phase space having the identical conserved energy.

Examples Dissipative systems are a special class of dynamical systems. Let us consider a few examples:

– For the damped mathematical pendulum Eq. (3.3) we find

$$\frac{\partial \dot{x}}{\partial x} = 0, \qquad \frac{\partial \dot{y}}{\partial y} = \frac{\partial[-\gamma y - \omega_0^2 \sin x]}{\partial y} = -\gamma \qquad \vec{\nabla}\cdot\dot{\boldsymbol{x}} = -\gamma \ < \ 0 \ .$$

The damped harmonic oscillator is consequently dissipative. It has a single fixpoint $(0,0)$ and the basin of attraction is the full phase space (modulo 2π). Some examples of trajectories and phase space evolution are illustrated in Fig. 3.1.

– For the non-linear rotator defined by Eq. (**??**) we have

$$\frac{\partial \dot{r}}{\partial r} + \frac{\partial \dot{\varphi}}{\partial \varphi} = \Gamma - 3r^2 = \begin{cases} < 0 \text{ for } \Gamma < 0 \\ < 0 \text{ for } \Gamma > 0 \ \text{ and } \ r > r_c/\sqrt{3} \\ > 0 \text{ for } \Gamma > 0 \ \text{ and } \ 0 < r < r_c/\sqrt{3} \end{cases} , \qquad (3.5)$$

where $r_c = \sqrt{\Gamma}$ is the radius of the limit cycle when $\Gamma > 0$. The system might either dissipate or take up energy, which is typical behavior of "adaptive systems" as we will discuss further in Sect. 3.1.3. Note that the phase space contracts both close to the fixpoint, for $\Gamma < 0$, and close to the limit cycle, for $\Gamma > 0$.

Phase Space Contraction and Coordinate Systems The time development of a small phase space volume, Eq. (3.4), depends on the coordinate system chosen to represent the variables. As an example we reconsider the non-linear rotator defined by Eq. (**??**) in terms of the Cartesian coordinates $x = r\cos\varphi$ and $y = r\sin\varphi$.

The respective infinitesimal phase space volumes are related via the Jacobian,

$$\mathrm{d}x\,\mathrm{d}y = r\,\mathrm{d}r\,\mathrm{d}\varphi \ ,$$

and we find

$$\frac{\dot{\Delta V}}{\Delta V} = \frac{\dot{r}\Delta r\Delta\varphi + r\dot{\Delta r}\Delta\varphi + r\Delta r\dot{\Delta\varphi}}{r\Delta r\Delta\varphi} = \frac{\dot{r}}{r} + \frac{\partial\dot{r}}{\partial r} + \frac{\partial\dot{\varphi}}{\partial\varphi} = 2\Gamma - 4r^2 \ ,$$

compare Eqs. (**??**) and (3.5). The amount and even the sign of the phase space contraction can depend on the choice of the coordinate system.

Divergence of the Flow and Lyapunov Exponents For a dynamical system $\dot{\mathbf{x}} = \mathbf{f}(\mathbf{x})$ the local change in phase space volume is given by the divergence of the flow

$$\frac{\Delta \dot{V}}{\Delta V} = \nabla \cdot \mathbf{f} = \sum_i \frac{\partial f_i}{\partial x_i} = \sum_i \lambda_i \tag{3.6}$$

and hence by the trace of the Jacobian $J_{ij} = \partial f_i / \partial x_j$, which we discussed in Sect. 3.1.2. The trace of a matrix corresponds to the sum $\sum_i \lambda_i$ of its eigenvalues λ_i. Phase space hence contracts when the sum of the local Lyapunov exponents is negative.

3.1.2 Strange Attractors and Dissipative Chaos

The Lorenz Model A rather natural question regards the possible existence of attractors with less regular behaviors, i.e. which are different from stable fixpoints, periodic or quasi-periodic motion. For this question we examine the Lorenz model

$$\begin{aligned} \dot{x} &= -\sigma(x-y), \\ \dot{y} &= -xz + rx - y, \\ \dot{z} &= xy - bz\ . \end{aligned} \tag{3.7}$$

The classical values are $\sigma = 10$ and $b = 8/3$, with r being the control variable.

Fixpoints of the Lorenz Model A trivial fixpoint is $(0,0,0)$. The non-trivial fixpoints are

$$\begin{aligned} 0 &= -\sigma(x-y), & x &= y, \\ 0 &= -xz + rx - y, & z &= r-1, \\ 0 &= xy - bz, & x^2 = y^2 &= b\,(r-1)\ . \end{aligned}$$

It is easy to see by linear analysis that the fixpoint $(0,0,0)$ is stable for $r < 1$. For $r > 1$ it becomes unstable and two new fixpoints appear:

$$C_{+,-} = \left(\pm\sqrt{b(r-1)}, \pm\sqrt{b(r-1)}, r-1\right)\ . \tag{3.8}$$

These are stable for $r < r_c = 24.74$ ($\sigma = 10$ and $b = 8/3$). For $r > r_c$ the behavior becomes more complicated and generally non-periodic.

Strange Attractors One can show, that the Lorenz model has a positive Lyapunov exponent for $r > r_c$. It is chaotic with sensitive dependence on the initial conditions. A typical orbit is illustrated in Fig. 3.2. The Lorenz model is at the same time dissipative, since

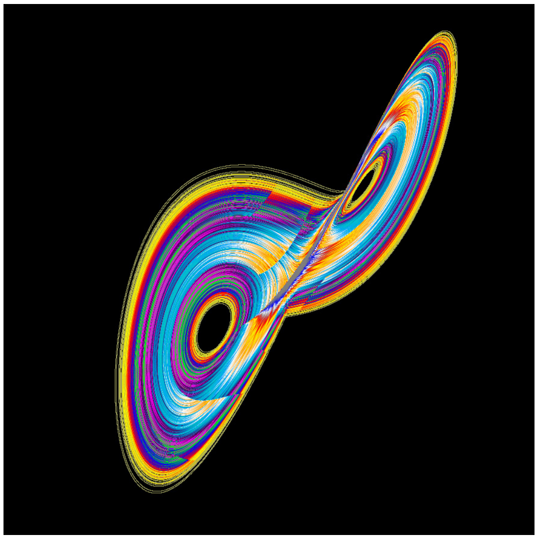

Fig. 3.2 A typical trajectory of the Lorenz system (3.7) for the classical set of parameters, $\sigma = 10$, $b = 8/3$ and $r = 28$. The chaotic orbit loops around the remnants of the two fixpoints (3.8), which are unstable for the selected set of parameters (color coded using ChaosPro)

$$\frac{\partial \dot{x}}{\partial x} + \frac{\partial \dot{y}}{\partial y} + \frac{\partial \dot{z}}{\partial z} = -(\sigma + 1 + b) \; < \; 0, \qquad \sigma > 0,\; b > 0 \; . \tag{3.9}$$

The attractor of the Lorenz system therefore cannot be a smooth surface. Close to the attractor the phase space contracts. At the same time two nearby orbits are repelled due to the positive Lyapunov exponents. One finds a self-similar structure for the Lorenz attractor with a fractal dimension 2.06 ± 0.01. Such a structure is called a *strange attractor*.

Dissipative Chaos and Strange Attractors Strange attractors can only occur in dynamical system of dimension three and higher, in one dimension fixpoints are the only possible attracting states and for limit cycles one needs at least two dimensions.

The Lorenz model has an important historical relevance in the development of chaos theory and is now considered a paradigmatic example of a chaotic system, since chaos in dissipative and deterministic dynamical systems is closely related to the emergence of strange attractors. Chaos may arise in one dimensional maps, as we have discussed in Sect. **??**, but continuous-time dynamical systems need to be at least three dimensional in order to show chaotic behavior.

Fractals Strange attractors often show a high degree of self-similarity, being fractal. Fractals can be defined on an abstract level by recurrent geometric rules, prominent examples are the Cantor set, the Sierpinski triangle and

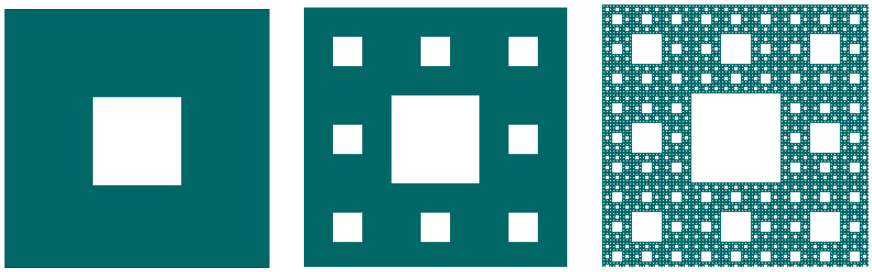

Fig. 3.3 The Sierpinski carpet and its iterative construction

the Sierpinski carpet illustrated in Fig. 3.3. Strange attractors are normally, strictly speaking, *multi fractal* i.e. fractals with a non-uniform self similarity.

The Hausdorff Dimension An important notion in the theory of fractals is the "Hausdorff dimension". We consider a geometric structure defined by a set of points in d dimensions and the number $N(l)$ of d-dimensional spheres of diameter l needed to cover this set. If $N(l)$ scales like

$$N(l) \propto l^{-D_H}, \qquad \text{for} \qquad l \rightarrow 0\,, \tag{3.10}$$

then D_H is called the Hausdorff dimension of the set. Alternatively we can rewrite Eq. (3.10) as

$$\frac{N(l)}{N(l')} = \left(\frac{l}{l'}\right)^{-D_H}, \qquad D_H = -\frac{\log[N(l)/N(l')]}{\log[l/l']}\,, \tag{3.11}$$

which is useful for self-similar structures (fractals).

The d-dimensional spheres necessary to cover a given geometrical structure will generally overlap. The overlap does not affect the value of the fractal dimension as long as the degree of overlap does not change qualitatively with decreasing diameter l.

The Hausdorff Dimension of the Sierpinski Carpet For the Sierpinski carpet we increase the number of points $N(l)$ by a factor of 8, compare Fig. 3.4, when we decrease the length scale l by a factor of 3 (see Fig. 3.3):

$$D_H \rightarrow -\frac{\log[8/1]}{\log[1/3]} = \frac{\log 8}{\log 3} \approx 1.8928\,.$$

3.1.3 Adaptive Systems

A general complex system is neither fully conserving nor fully dissipative. Adaptive systems will have phases where they take up energy and periods

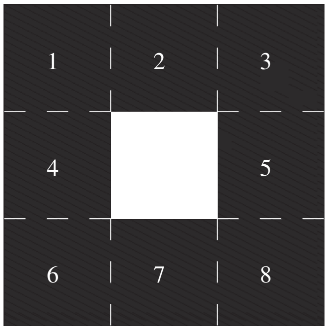

Fig. 3.4 The fundamental unit of the Sierpinski carpet, compare Fig. 3.3, contains eight squares which can be covered by discs of an appropriate diameter

where they give energy back to the environment. An example is the non-linear rotator of Eq. (**??**), see also Eq. (3.5).

In general one affiliates with the term "adaptive system" the notion of complexity and adaption. Strictly speaking any dynamical system is adaptive if $\nabla \cdot \dot{\boldsymbol{x}}$ may take both positive and negative values. In practice, however, it is usual to reserve the term adaptive system to dynamical systems showing a certain complexity, such as emerging behavior.

The Van der Pol Oscillator Circuits or mechanisms built for the purpose of controlling an engine or machine are intrinsically adaptive. An example is the van der Pol oscillator,

$$\ddot{x} - \epsilon(1-x^2)\dot{x} + x = 0, \qquad \begin{array}{l} \dot{x} = y \\ \dot{y} = \epsilon(1-x^2)y - x \end{array} \tag{3.12}$$

where $\epsilon > 0$ and where we have used the phase space variables $\boldsymbol{x} = (x, y)$. We evaluate the time evolution $\vec{\nabla} \cdot \dot{\boldsymbol{x}}$ of the phase-space volume,

$$\vec{\nabla} \cdot \dot{\boldsymbol{x}} = +\epsilon\,(1-x^2)\ .$$

The oscillator takes up/dissipates energy for $x^2 < 1$ and $x^2 > 1$, respectively. A simple mechanical example for a system with similar properties is illustrated in Fig. 3.5

Secular Perturbation Theory We consider a perturbation expansion in ϵ. The solution of Eq. (3.12) is

$$x_0(t) = a\, e^{i(\omega_0 t + \phi)} + c.c., \qquad \omega_0 = 1\ , \tag{3.13}$$

for $\epsilon = 0$. We note that the amplitude a and phase ϕ are arbitrary in Eq. (3.13). The perturbation $\epsilon(1-x^2)\dot{x}$ might change, in principle, also the given frequency $\omega_0 = 1$ by an amount $\propto \epsilon$. In order to account for this "secular perturbation" we make the ansatz

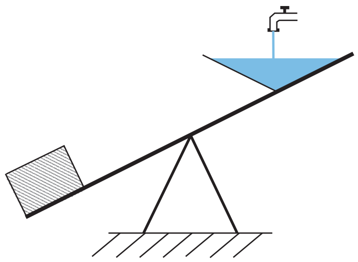

Fig. 3.5 The seesaw with a water container at one end; an example of an oscillator that takes up and disperses energy periodically

$$x(t) = \left[A(T)e^{it} + A^*(T)e^{-it}\right] + \epsilon x_1 + \cdots , \qquad A(T) = A(\epsilon t) , \tag{3.14}$$

which differs from the usual expansion $x(t) \to x_0(t) + \epsilon x'(t) + \cdots$ of the full solution $x(t)$ of a dynamical system with respect to a small parameter ϵ.

Expansion From Eq. (3.14) we find to the order $O(\epsilon^1)$

$$\begin{aligned}
x^2 &\approx A^2 e^{2it} + 2|A|^2 + (A^*)^2 e^{-2it} + 2\epsilon x_1 \left[Ae^{it} + Ae^{-it}\right] \\
\epsilon(1-x^2) &\approx \epsilon(1-2|A|^2) - \epsilon\left[A^2e^{2it} + (A^*)^2 e^{-2it}\right] , \\
\dot{x} &\approx \left[(\epsilon A_T + iA)\, e^{it} + c.c.\right] + \epsilon\, \dot{x}_1, \qquad A_T = \frac{\partial A(T)}{\partial T} \\
\epsilon(1-x^2)\dot{x} &= \epsilon(1-2|A|^2)\left[iAe^{it} - iA^*e^{-it}\right] \\
&\quad - \epsilon\left[A^2e^{2it} + (A^*)^2e^{-2it}\right]\left[iAe^{it} - iA^*e^{-it}\right]
\end{aligned}$$

and

$$\begin{aligned}
\ddot{x} &= \left[\left(\epsilon^2 A_{TT} + 2i\epsilon A_T - A\right) e^{it} + c.c.\right] + \epsilon\, \ddot{x}_1 \\
&\approx \left[(2i\epsilon A_T - A)\, e^{it} + c.c.\right] + \epsilon \ddot{x}_1 \ .
\end{aligned}$$

Substituting these expressions into Eq. (3.12) we obtain in the order $O(\epsilon^1)$

$$\ddot{x}_1 + x_1 = \left(-2iA_T + iA - i|A|^2 A\right) e^{it} - iA^3 e^{3it} + c.c. \ . \tag{3.15}$$

The Solvability Condition Equation (3.15) is identical to a driven harmonic oscillator, which will be discussed in Chap. **??** in more detail. The time dependencies

$$\sim e^{it} \qquad \text{and} \qquad \sim e^{3it}$$

of the two terms on the right-hand side of Eq. (3.15) are proportional to the unperturbed frequency $\omega_0 = 1$ and to $3\omega_0$, respectively.

The term $\sim e^{it}$ is therefore exactly at resonance and would induce a diverging response $x_1 \to \infty$, in contradiction to the perturbative assumption made by ansatz (3.14). Its prefactor must therefore vanish:

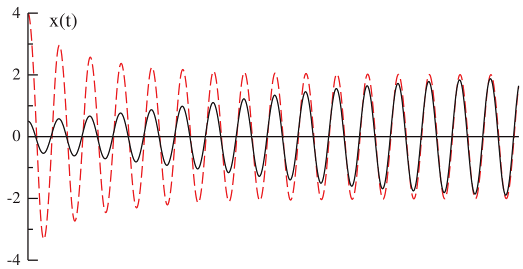

Fig. 3.6 Two solutions of the van der Pol oscillator, Eq. (3.12), for small ϵ and two different initial conditions. Note the self-generated amplitude stabilization

$$A_T = \frac{\partial A}{\partial T} = \frac{1}{2}\left(1-|A|^2\right) A, \qquad \frac{\partial A}{\partial t} = \frac{\epsilon}{2}\left(1-|A|^2\right) A\ , \tag{3.16}$$

where we have used $T = \epsilon t$. The solubility condition Eq. (3.16) can be written as

$$\dot a\, e^{i\phi} + i\dot\phi\, a\, e^{i\phi} = \frac{\epsilon}{2}\left(1-a^2\right) a\, e^{i\phi}$$

in phase-magnitude representation $A(t) = a(t)e^{i\phi(t)}$, or

$$\begin{aligned} \dot a &= \epsilon\left(1-a^2\right) a/2, \\ \dot\phi &\sim O(\epsilon^2)\ . \end{aligned} \tag{3.17}$$

The system takes up energy for $a < 1$ and the amplitude a increases until the saturation limit $a \to 1$, the conserving point. For $a > 1$ the system dissipates energy to the environment and the amplitude a decreases, approaching unity for $t \to \infty$, just as we discussed in connection with Eq. (**??**).

The solution $x(t) \approx 2\,a\cos(t)$, compare Eqs. (3.14) and (3.17), of the van der Pol equations therefore constitutes an amplitude-regulated oscillation, as illustrated in Fig. 3.6. This behavior was the technical reason for historical development of the control systems that are described by the van der Pol equation (3.12).

Liénard Variables For large ϵ it is convenient to define, compare Eq. (3.12), with

$$\epsilon\frac{\mathrm{d}}{\mathrm{d}t}Y(t) = \ddot x(t) - \epsilon\left(1-x^2(t)\right)\dot x(t) = -x(t) \tag{3.18}$$

or

$$\epsilon\dot Y = \ddot X - \epsilon\left(1-X^2\right)\dot X, \qquad X(t) = x(t),$$

the Liénard variables $X(t)$ and $Y(t)$. Integration of $\dot Y$ with respect to t yields

$$\epsilon Y = \dot X - \epsilon\left(X - \frac{X^3}{3}\right)\ ,$$

where we have set the integration constant to zero. We obtain, together with Eq. (3.18),

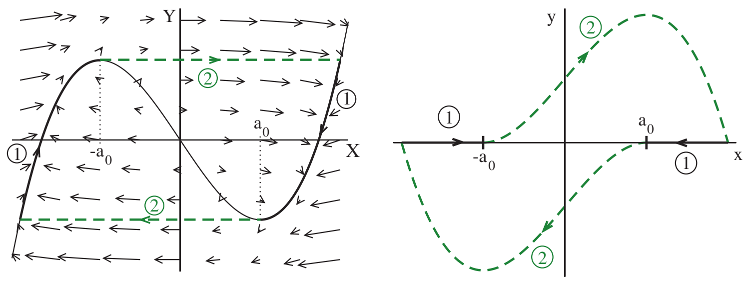

Fig. 3.7 The Van der Pol oscillator for a large driving $c \equiv \epsilon$. *Left*: The relaxation oscillations with respect to the Liénard variables Eq. (3.19). The *arrows* indicate the flow $(\dot{X}, \dot{Y})$, for $c = 3$, see Eq. (3.19). Also shown is the $\dot{X} = 0$ isocline $Y = -X + X^3/3$ (*solid line*) and the limit cycle, which includes the *dashed line with an arrow* and part of the isocline. *Right*: The limit cycle in terms of the original variables $(x, y) = (x, \dot{x}) = (x, v)$. Note that $X(t) = x(t)$

$$\begin{aligned} \dot{X} &= c\Big(Y - f(X)\Big) \\ \dot{Y} &= -X/c \end{aligned} \qquad f(X) = X^3/3 - X \;, \tag{3.19}$$

where we have set $c \equiv \epsilon$, as we are now interested in the case $c \gg 1$.

Relaxation Oscillations We discuss the solution of the van der Pol oscillator Eq. (3.19) for a large driving c graphically, compare Fig. 3.7, by considering the flow $(\dot{X}, \dot{Y})$ in phase space (X, Y). For $c \gg 1$ there is a separation of time scales,

$$(\dot{X}, \dot{Y}) \;\sim\; (c, 1/c), \qquad \dot{X} \gg \dot{Y} \;,$$

which leads to the following dynamical behavior:

- Starting at a general $(X(t_0), Y(t_0))$ the orbit develops very fast $\sim c$ and nearly horizontally until it hits the "isocline"[1]

$$\dot{X} = 0, \qquad Y = f(X) = -X + X^3/3 \;. \tag{3.20}$$

- Once the orbit is close to the $\dot{X} = 0$ isocline $Y = -X + X^3/3$ the motion slows down and it develops slowly, with a velocity $\sim 1/c$ close-to (but not exactly on) the isocline (Eq. (3.20)).
- Once the slow motion reaches one of the two local extrema $X = \pm a_0 = \pm 1$ of the isocline, it cannot follow the isocline any more and makes a rapid transition towards the other branch of the $\dot{X} = 0$ isocline, with $Y \approx$ const. Note, that trajectories may cross the isocline vertically, e.g. right at the extrema $\dot{Y}|_{X=\pm 1} = \mp 1/c$ is small but finite.

The orbit therefore relaxes rapidly towards a limiting oscillatory trajectory, illustrated in Fig. 3.7, with the time needed to perform a whole oscillation depending on the relaxation constant c; therefore the term "relaxation oscilla-

[1] The term isocline stands for "equal slope" in ancient Greek.

tion". Relaxation oscillators represent an important class of cyclic attractors, allowing to model systems going through several distinct and well characterized phases during the course of one cycle. We will discuss relaxation oscillators further in Chap. **??**.

3.1.4 Conserving Adaptive Systems

A conserving dynamical system per definition conserves the volume of phase space enclosed by a set of trajectories, as discussed in Sect. 3.1.1. The phase space volume expands and contracts, on the other hand, alternatingly for adaptive systems. This is the case, e.g., for the Van der Pol oscillator, as defined by Eq. (3.12), and for the Taken-Bogdanov system, which we investigated in Sect. **??**.

An adaptive system can hence not conserve phase-space volume, but it may dispose of conserved quantities, constants of motions.

Energy Conservation in Mechanical Systems Newton's equation

$$\begin{aligned} \dot{\mathbf{x}} &= \mathbf{v} \\ \dot{\mathbf{v}} &= -\nabla V(\mathbf{x}) \end{aligned} \qquad\qquad E(\mathbf{x},\mathbf{v}) = \frac{\mathbf{v}^2}{2} + V(\mathbf{x}) \tag{3.21}$$

for a mechanical systems with a potential $V(\mathbf{x})$ conserves the energy E,

$$\frac{dE}{dt} = \frac{\partial E}{\partial \mathbf{x}}\dot{\mathbf{x}} + \frac{\partial E}{\partial \mathbf{v}}\dot{\mathbf{v}} = \big(\nabla V + \dot{\mathbf{v}}\big)\mathbf{v} = 0 \ .$$

The energy is an instance of a *constant of motion*, a conserved quantity.

Lotka-Volterra Model for Rabbits and Foxes Evolution equations for one or more interacting species are termed *Lotka-Volterra* models. A basic example is that of a prey (rabbit) with population density x being hunted by a predator (fox) with population density y,

$$\begin{array}{rl} \dot{x} = & Ax - Bxy \\ \dot{y} = & -Cy + Dxy \end{array} \ . \tag{3.22}$$

The population x of rabbits can grow by themselves but the foxes need to eat rabbits in order to multiply. All constants A, B, C and D are positive.

Fixpoints The Lotka-Volterra equation (3.22) has two fixpoints,

$$\mathbf{x}_0^* \ = (0,0), \qquad\qquad \mathbf{x}_1^* \ = (C/D, A/B) \ . \tag{3.23}$$

with the respective Jacobians, compare Sect. **??**,

$$J_0 = \begin{pmatrix} A & 0 \\ 0 & -C \end{pmatrix} \ , \qquad\qquad J_1 = \begin{pmatrix} 0 & -BC/D \\ AD/B & 0 \end{pmatrix} \ .$$

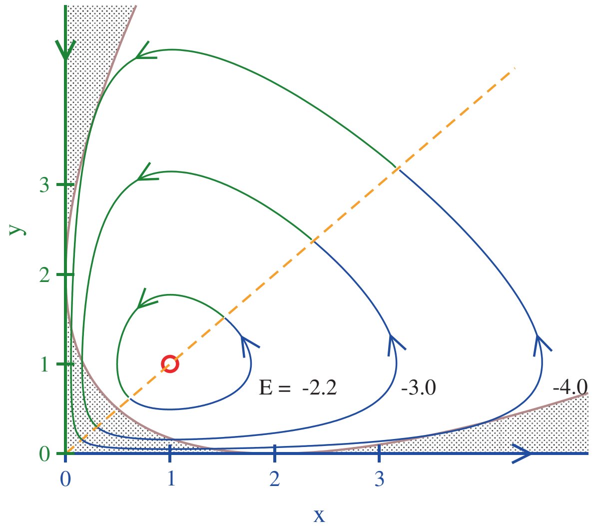

Fig. 3.8 The phase space flow of the fox and rabbit Lotka-Volterra model (3.22) For $x > y$ / $x < y$ the flow, expands/contracts (*blue/green orbits*) according to (3.24). The trajectories coincide with the iso-energy lines of the conserved function E on phase space, Eq. (3.25). The fixpoints are the saddle $(0, 0)$ and the neutral focus $(1, 1)$ (*open red circle*). The Lyapunov exponents are real in the shaded region and complex otherwise, with the separatrix given by expression (3.27)

The trivial fixpoint $\mathbf{x}_0^*$ is hence a saddle and $\mathbf{x}_1^*$ a neutral focus with purely imaginary Lyapunov exponents $\lambda = \pm i\sqrt{CA}$. The trajectories circling the focus close onto themselves, as illustrated in Fig. 3.8 for $A = B = C = D = 1$.

Phase space Evolution We now consider the evolution of phase space volume, as defined by Eq. (3.4),

$$\frac{\partial \dot{x}}{\partial x} + \frac{\partial \dot{v}}{\partial v} = A - By - C + Dx \; . \tag{3.24}$$

The phase space expands/contracts for y smaller/larger than $(A+Dx-C)/B$, the tell sign of an adaptive system.

Constant of Motion The function

$$E(x, y) = A\log(y) + C\log(x) - By - Dx \tag{3.25}$$

on phase space (x, y) is a constant of motion for the Lotka-Volterra model (3.22), since

$$\begin{aligned}\frac{dE}{dt} &= A\dot{y}/y + C\dot{x}/x - B\dot{y} - D\dot{x} \\ &= A(-C + Dx) + C(A - By) - B(-C + Dx)y - D(A - By)x \\ &= (A - By)(-C + Dx) + (A - By)(C - Dx) = 0 \; .\end{aligned}$$

The prey-predator system (3.22) does hence dispose of a non-trivial constant of motion. Note that $E(x, y)$ has no biological significance which would be evident per se.

Iso-Energy Manifolds The flow of a $d-$dimensional dynamical system $\dot{\mathbf{x}} = \mathbf{f}(\mathbf{x})$ disposing of a conserved functional $E(\mathbf{x})$, we call it here a generalized energy, is always restricted to an iso-energy manifold defined by $E(\mathbf{x}) =$ const,

$$\frac{dE}{dt} = \nabla E \cdot \dot{\mathbf{x}} = 0 \; . \qquad \nabla E \perp \dot{\mathbf{x}} \tag{3.26}$$

The flow $\dot{\mathbf{x}}$ is hence perpendicular to the gradient ∇E of the conserved generalized energy and hence confined to an iso-energy manifold. The phase space of the fox and rabbit Lotka-Volterra model is two-dimensional and the iso-energy lines are hence one-dimensional, coinciding therefore with the trajectories, as illustrated in Fig. 3.8

Lyapunov Exponent We consider $A = B = C = D = 1$ and the Jacobian

$$\begin{pmatrix} (1-y) & -x \\ y & (x-1) \end{pmatrix}, \qquad \lambda_\pm = \frac{x-y}{2} \pm \frac{1}{2}\sqrt{(x-y)^2 - 4(x+y-1)}$$

for a generic point (x, y) in phase space. The Lyapunov exponents $\lambda_\pm$ are real close to the axes and complex further away, with the separatrix given by

$$(x-y)^2 = 4(x+y-1), \qquad y = x + 2 \pm \sqrt{8x} \; . \tag{3.27}$$

There is no discernible change in the flow dynamics across the separatrix (3.27), which we have included in Fig. 3.8, viz when the Lyapunov exponents acquire finite imaginary components.

Invariant Manifolds Fixpoints and limit cycles are examples of invariant subsets of phase space.

> Invariant Manifold. A subset M of phase space invariant under the flow for all times $t \in [-\infty, \infty]$ is denoted an *invariant manifold*.

All trajectories of the fox and rabbit Lotka-Volterra model, apart from the stable and the unstable manifolds of the saddle $(0, 0)$, are closed and constitute hence invariant manifolds.

Fixpoints and limit cycles are invariant manifolds with dimensions zero and one respectively, strange attractors, see Sect. 3.1.1, have generically a fractal dimension.

Invariant Manifolds and Averaged Lyapunov Exponents The evolution of phase space on an invariant manifold (viz inside the manifold) with dimension m is determined by m Lyapunov exponents whenever the manifold has a smooth topology (which is not the case for fractals).

Overall the phase space cannot expand or contract for bounded invariant manifolds M and one has hence m Lyapunov exponents for which the real part vanishes when averaged of over the M.

This is the case for all trajectories of the fox and rabbit Lotka-Volterra model and manifestly evident for the case $A = B = C = D = 0$ discussed above, for which the real part of the Lyapunov exponent $\lambda_\pm$ is anti-symmetric under the exchange $x \leftrightarrow y$.

Lotka-Volterra system with resource limitation The reproduction of the prey in the original Lotka-Volterra model (3.22) is not limited. In practice, the population density x of the rabbits will be bounded by the carrying capacity x_{max} of the supporting environment, such that $x < x_{\text{max}}$. The modified model,

$$\dot{x} = Ax\left(1 - \frac{x}{x_{\text{max}}}\right) - Bxy, \qquad \dot{y} = (Dx - C)y\,.$$

has the non-trival fixpoint

$$x^* = \frac{C}{D}, \qquad y^* = \frac{A}{B}\left(1 - \frac{C}{Dx_{\text{max}}}\right), \tag{3.28}$$

which exists for $C < Dx_{\text{max}}$. The population of rabits is never large enough to support the a finite population of foxes in the opposite case, when $C > Dx_{\text{max}}$, which leads to $x \to x_{\text{max}}$ and $y \to 0$. When existing, the steady state defined by (3.28) is stable.

3.2 Diffusion and Transport

Deterministic vs. Stochastic Time Evolution So far we have discussed some concepts and examples of deterministic dynamical systems, governed by sets of coupled differential equations without noise or randomness. At the other extreme are diffusion processes for which the random process dominates the dynamics.

Dissemination of information through social networks is one of many examples where diffusion processes plays a paramount role. The simplest model of diffusion is the Brownian motion, which is the erratic movement of grains suspended in liquid observed by the botanist Robert Brown as early as 1827. Brownian motion became the prototypical example of a stochastic process after the seminal works of Einstein and Langevin at the beginning of the twentieth century.

3.2.1 Random Walks, Diffusion and Lévy Flights

One-Dimensional Diffusion We consider the random walk of a particle along a line, with the equal probability 1/2 to move left/right at every time step. The probability

$$p_t(x), \qquad x = 0, \pm 1, \pm 2, \dots, \qquad t = 0, 1, 2, \dots$$

to find the particle at time t at position x obeys the master equation

$$p_{t+1}(x) = \frac{p_t(x-1) + p_t(x+1)}{2} \,. \tag{3.29}$$

In order to obtain the limit of continuous time and space, we consider explicitly the steps Δx and Δt in space and time, and rewrite the master equation (3.29) as

$$\frac{p_{t+\Delta t}(x) - p_t(x)}{\Delta t} = \frac{(\Delta x)^2}{2\Delta t} \, \frac{p_t(x+\Delta x) + p_t(x-\Delta x) - 2p_t(x)}{(\Delta x)^2} \,, \tag{3.30}$$

where we have subtracted on both sides the current distribution $p_t(x)$. Now, taking the limit $\Delta x, \Delta t \to 0$ in such a way that $(\Delta x)^2/(2\Delta t)$ remains finite, we obtain the diffusion equation

$$\frac{\partial p(x,t)}{\partial t} = D \, \frac{\partial^2 p(x,t)}{\partial x^2}, \qquad D = \frac{(\Delta x)^2}{2\Delta t} \,, \tag{3.31}$$

with D being denoted the diffusion constant.

Solution of the Diffusion Equation The solution of the diffusion equation (3.31) is given by

$$\Phi(x,t) = \frac{1}{\sqrt{4\pi D t}} \exp\left(-\frac{x^2}{4Dt}\right), \qquad \int_{-\infty}^{\infty} \mathrm{d}x \, \Phi(x,t) = 1 \,, \tag{3.32}$$

for a localized initial state[2] $\Phi(x, t=0) = \delta(x)$, as can been seen using

$$\dot{\Phi} = \frac{-\Phi}{2t} + \frac{x^2 \Phi}{4Dt^2}, \qquad \Phi' = \frac{-x\Phi}{2Dt}, \qquad \Phi'' = \frac{-\Phi}{2Dt} + \frac{x^2\Phi}{4D^2t^2} \,.$$

and the diffusion equation (3.31).

Diffusive Transport Equation (3.32) corresponds, as a function of the coordinate x, to a Gaussian, see Sect. **??**, with variance $\sigma^2 = 2Dt$. One hence concludes that the variance of the displacement follows diffusive behavior, i.e.

$$\langle x^2(t) \rangle = 2D\,t \,, \qquad \bar{x} = \sqrt{\langle x^2(t) \rangle} = \sqrt{2D\,t} \,. \tag{3.33}$$

[2] Note: $\int e^{-x^2/a} \mathrm{d}x = \sqrt{a\pi}$ and $\lim_{a\to 0} \exp(-x^2/a)/\sqrt{a\pi} = \delta(x)$.

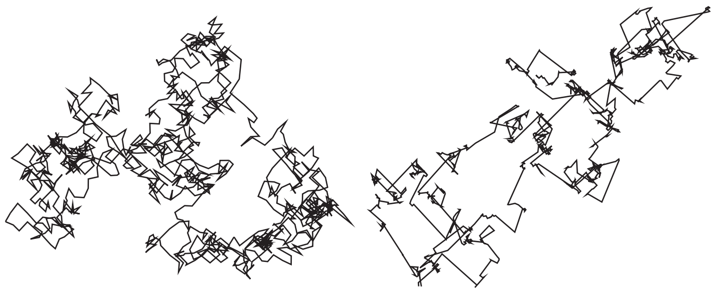

Fig. 3.9 Examples of random walkers with scale-free distributions $\sim |\Delta x|^{1+\beta}$ for the real-space jumps, see Eq. (3.35). *Left*: $\beta = 3$, which falls into the universality class of standard Brownian motion. *Right*: $\beta = 0.5$, a typical Levy flight. Note the occurrence of longer-ranged jumps in conjunction with local walking

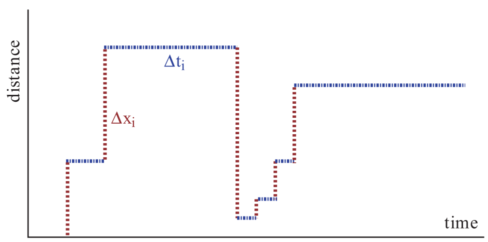

Fig. 3.10 A random walker with distributed waiting times Δt_i and jumps Δx_i may become a generalized Lévy flight, compare Eq. 3.35

Diffusive transport is characterized by transport sublinear in time in contrast to ballistic transport with $x = vt$, as illustrated in Fig. 3.9.

Green's Function for Diffusion For general initial distributions $p_0(x) = p(x, 0)$ of walkers the diffusion equation (3.31) is solved by

$$p(x,t) = \int dy\, \Phi(x-y,t)\, p_0(y) \ , \tag{3.34}$$

since $\lim_{t\to 0} \Phi(x-y,t) = \delta(x-y)$. An integral kernel which allows to construct the solution of a differential equation for arbitrary initial conditions is denoted a *Green's function*.

Lévy Flights We can generalize the concept of a random walker, which is at the basis of ordinary diffusion, and consider a random walk with distributions $p(\Delta t)$ and $p(\Delta x)$ for waiting times Δt_i and jumps Δx_i, at every step $i = 1,\ 2, \ldots$ of the walk, as illustrated in Fig. 3.10. One may assume scale-free distributions

$$p(\Delta t) \ \sim \ \frac{1}{(\Delta t)^{1+\alpha}}, \qquad p(\Delta x) \ \sim \ \frac{1}{(\Delta x)^{1+\beta}}, \qquad \alpha, \beta > 0 \ . \tag{3.35}$$

If $\alpha > 1$ (finite mean waiting time) and $\beta > 2$ (finite variance), nothing special happens. In this case the central limiting theorem for well behaved distribution functions is valid for the spatial component and one obtains standard Brownian diffusion. Relaxing the above conditions one finds four regimes: normal Brownian diffusion, "Lévy flights", fractional Brownian motion, also denoted "subdiffusion" and generalized Lévy flights termed "ambivalent processes". Their respective scaling laws are listed in Table 3.1 and two examples are shown in Fig. 3.9.

Lévy flights occur in a wide range of processes, such as in the flight patterns of wandering albatrosses or in human travel habits, which seem to be characterized by a generalized Lévy flight with $\alpha, \beta \approx 0.6$.

3.2.2 Markov Chains

For many common stochastic processes $x_1 \to x_2 \to x_3 \to \dots$ the probability to visit a state $x_{t+1} = y$ depends solely on the current state $x_t = x$.

Markov Property. A stochastic process is *markovian* if it has no memory.

A memory would be present, on the other hand, if the transition rule $x_t \to x_{t+1}$ would be functionally dependent on earlier x_{t-1}, x_{t-2}, ... elements of the process.

Absorbing States The transition probabilities $p(x, y)$ to visit a state $x_{t+1} = y$, when being at $x_t = x$, are normalized,

$$1 = \sum_y p(x,y), \qquad p(x,y) \geq 0 \ , \tag{3.36}$$

since one always arrives to some state $x_{t+1} = y$ when starting from a given $x_t = x$. Note, that $p(x, x) > 0$ is possible and a state x^* is called *absorbing* whenever

$$p(x^*, x^*) = 1, \qquad p(x^*, y) = 0, \qquad \forall y \neq x^* \ . \tag{3.37}$$

Table 3.1 The four regimes of a generalized walker with distribution functions, Eq. (3.35), characterized by scalings $\propto (\Delta t)^{-1-\alpha}$ and $\propto (\Delta x)^{-1-\beta}$ for the waiting times Δt and jumps Δx, as depicted in Fig. 3.10

$\alpha > 1$	$\beta > 2$	$\bar{x} \sim \sqrt{t}$	Ordinary diffusion
$\alpha > 1$	$0 < \beta < 2$	$\bar{x} \sim t^{1/\beta}$	Lévy flights
$0 < \alpha < 1$	$\beta > 2$	$\bar{x} \sim t^{\alpha/2}$	Subdiffusion
$0 < \alpha < 1$	$0 < \beta < 2$	$\bar{x} \sim t^{\alpha/\beta}$	Ambivalent processes

The stochastic process can be viewed as being terminated or *extinct* when reaching an absorbing state. The extinction probability is then the probability to hit x^* when starting from a given state x_0. A famous example is the Galton-Watson process discussed in Chap. **??**, which describes the extinction probabilities of family names.

Master Equation We consider now density distributions $\rho_t(x)$ of walkers with identical transition probabilities $p(x,y)$ and discrete times $t = 0, 1, \ldots$. The evolution equation for the density of walkers,

$$\begin{aligned}
\rho_{t+1}(y) &= \rho_t(y) + \textstyle\sum_x \big[\, \rho_t(x)p(x,y) - \rho_t(y)p(y,x) \,\big] \\
&= \rho_t(y) + \textstyle\sum_x \rho_t(x)p(x,y) - \rho_t(y) \\
&= \textstyle\sum_x \rho_t(x)p(x,y)
\end{aligned} \tag{3.38}$$

describes the conservation of the number of walkers, where we have used (3.36), and is denoted *master equation*. Random walks, compare Eq. (3.29), and any other stochastic time series, e.g. as discussed in Chap. **??**, are described by master equations.

Stationarity A Markov process becomes stationary when the distribution of walkers does not change anymore with time, viz when

$$\rho^*(y) = \rho_{t+1}(y) = \rho_t(y), \qquad \sum_x \rho^*(x)p(x,y) = \rho^*(y), \qquad \rho^* P = \rho^* \ ,$$

where we have defined with P the matrix $p(x,y)$. The stationary distribution of walkers ρ^* is then a left eigenvector of P.

General Two-State Markov Process As an example we define with, compare Fig. 3.11,

$$P = \begin{pmatrix} \alpha & 1-\alpha \\ 1-\beta & \beta \end{pmatrix}, \qquad \alpha, \beta \in [0,1] \tag{3.39}$$

the transition matrix P for the general two-state Markov process. The eigenvalues λ of the left eigenvectors $\rho^* = (\rho(1), \rho(2))$ of P are determined by

$$\begin{aligned}
\alpha\,\rho(1) + (1-\beta)\rho(2) &= \lambda\rho(1) \\
(1-\alpha)\rho(1) + \qquad \beta\,\rho(2) &= \lambda\rho(2)
\end{aligned} \ , \tag{3.40}$$

which has the solutions

$$\lambda_1 = 1, \qquad \rho^*_{\lambda_1} = \frac{1}{N_1}\begin{pmatrix} 1-\beta \\ 1-\alpha \end{pmatrix}, \qquad N_1 = \sqrt{(1-\alpha)^2 + (1-\beta)^2}$$

and

$$\lambda_2 = \alpha + \beta - 1, \qquad \rho^*_{\lambda_2} = \frac{1}{\sqrt{2}}\begin{pmatrix} 1 \\ -1 \end{pmatrix} \ .$$

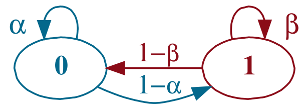

Fig. 3.11 The general two-state Markov chain, as defined by Eq. (3.39)

The first eigenvalue dominates generically, $\lambda_1 = 1 > |\alpha+\beta-1| = |\lambda_2|$, with the contribution to $\rho^*_{\lambda_2}$ dying out. All walkers will end up in an absorbing state whenever one is present. E.g. for $\alpha = 1$ the stationary distribution $\rho^*_1 = (1,0)$.

Random Surfer Model A famous diffusion process is the "random surfer model" which tries to capture the behavior of Internet users. This model is at the basis of the original Page & Brin Google page-rank algorithm.

Consider a network of $i = 1,\dots,N$ Internet hosts connected by directed hyperlinks characterized by the adjacency matrix A_{ij}, as defined in Chap. **??**. We denote with

$$\rho_i(t), \qquad \sum_{i=1}^{N} \rho_i(t) = 1$$

the probability of finding, at any given time t, an Internet surfer visiting the host i. The surfers are assumed to perform a markovian walk on the Internet by clicking randomly any available out-going hyperlink, giving raise to the master equation

$$\rho_i(t+1) = \frac{c}{N} + (1-c)\sum_j \frac{A_{ij}}{\sum_l A_{lj}}\rho_j(t)\ . \tag{3.41}$$

Normalization is conserved,

$$\sum_i \rho_i(t+1) = c + (1-c)\sum_j \frac{\sum_i A_{ij}}{\sum_l A_{lj}}\rho_j(t) = c + (1-c)\sum_j \rho_j(t)\ .$$

Hence $\sum_i \rho_i(t+1) = 1$ whenever $\sum_j \rho_j(t) = 1$.

The Google page rank The parameter c in the random surfer model regulates the probability to randomly enter the Internet:

– For $c = 1$ the adjacency matrix and hence the hyperlinks are irrelevant. We can interpret therefore c as the uniform probability to enter the Internet.
– For $c = 0$ a surfer never enters the Internet randomly, he continues to click around forever. $1-c$ is hence the probability to stop clicking hyperlinks.

The random surfer model (3.41) can be solved iteratively. Convergence is fast for not too small c. At every iteration authority is transferred from one host j to other hosts i through its outgoing hyperlinks A_{ij}. The steady-state density

ρ_i of surfers can hence be considered as a measure of host authority and is equivalent to the Google page rank.

Relation to Graph Laplacian The continuous time version of the random surfer model can be derived, for the case $c = 0$, from

$$\frac{\rho_i(t+\Delta t)-\rho_i(t)}{\Delta t} = \sum_j \frac{A_{ij}}{k_j}\rho_j(t) \,-\, \rho_i(t), \qquad k_j = \sum_l A_{lj} \ ,$$

where k_j is the out-degree of host j and $\Delta t = 1$ initially. Taking now the limit $\Delta t \to 0$ we obtain

$$\frac{d}{dt}\rho = \tilde{\Lambda}\,\rho, \qquad \tilde{\Lambda}_{ij} = -\frac{\Lambda_{ij}}{k_j}, \qquad \Lambda_{ij} = k_j\delta_{ij} - A_{ij} \ , \tag{3.42}$$

where Λ_{ij} is the Graph Laplacian discussed in Chap. **??**. Equation (3.42) corresponds to the generalization of the diffusion equation (3.31) to networks.

3.2.3 The Langevin Equation and Diffusion

Diffusion as a Stochastic Process Langevin proposed to describe the diffusion of a particle by the stochastic differential equation

$$m\,\dot{v} = -m\,\gamma\,v \,+\, \xi(t), \qquad \langle\xi(t)\rangle = 0, \qquad \langle\xi(t)\xi(t')\rangle = Q\delta(t-t'), \tag{3.43}$$

where $v(t)$ is the velocity of the particle and $m > 0$ its mass.

(i) The term $-m\gamma v$ on the right-hand-side of Eq. (3.43) corresponds to a damping term, the friction being proportional to $\gamma > 0$.
(ii) $\xi(t)$ is a stochastic variable, viz noise. The brackets $\langle\ldots\rangle$ denote ensemble averages, i.e. averages over different noise realizations.
(iii) As *white noise* (in contrast to *colored noise*) one denotes noise with a flat power spectrum (as white light), viz $\langle\xi(t)\xi(t')\rangle \propto \delta(t-t')$.
(iv) The constant Q is a measure for the strength of the noise.

Solution of the Langevin Equation Considering a specific noise realization $\xi(t)$, one finds

$$v(t) = v_0\,e^{-\gamma t} \,+\, \frac{e^{-\gamma t}}{m}\int_0^t \mathrm{d}t'\,e^{\gamma t'}\,\xi(t') \tag{3.44}$$

for the solution of the Langevin equation (3.43), where $v_0 \equiv v(0)$.

Mean Velocity For the ensemble average $\langle v(t)\rangle$ of the velocity one finds

$$\langle v(t)\rangle = v_0\, e^{-\gamma t} \,+\, \frac{e^{-\gamma t}}{m} \int_0^t \mathrm{d}t'\, e^{\gamma t'} \underbrace{\langle \xi(t')\rangle}_{0} = \; v_0\, e^{-\gamma t} \;. \tag{3.45}$$

The average velocity decays exponentially to zero.

Mean Square Velocity For the ensemble average $\langle v^2(t)\rangle$ of the velocity squared one finds

$$\begin{aligned}
\langle v^2(t)\rangle \;&=\; v_0^2\, e^{-2\gamma t} \,+\, \frac{2\, v_0\, e^{-2\gamma t}}{m} \int_0^t \mathrm{d}t'\, e^{\gamma t'} \underbrace{\langle \xi(t')\rangle}_{0} \\
&\quad + \frac{e^{-2\gamma t}}{m^2} \int_0^t \mathrm{d}t' \int_0^t \mathrm{d}t''\, e^{\gamma t'}\, e^{\gamma t''} \underbrace{\langle \xi(t')\xi(t'')\rangle}_{Q\,\delta(t'-t'')} \\
&=\; v_0^2\, e^{-2\gamma t} \,+\, \frac{Q\, e^{-2\gamma t}}{m^2} \underbrace{\int_0^t \mathrm{d}t'\, e^{2\gamma t'}}_{(e^{2\gamma t}-1)/(2\gamma)}
\end{aligned}$$

and finally

$$\langle v^2(t)\rangle = v_0^2\, e^{-2\gamma t} \,+\, \frac{Q}{2\,\gamma\, m^2} \left(1 - e^{-2\gamma t}\right) \;. \tag{3.46}$$

For long times the average squared velocity

$$\lim_{t\to\infty} \langle v^2(t)\rangle = \frac{Q}{2\,\gamma\, m^2} \tag{3.47}$$

becomes, as expected, independent of the initial velocity v_0. Equation (3.47) shows explicitly that the dynamics is driven exclusively by the stochastic process $\propto Q$ for long time scales.

The Langevin Equation and Diffusion The Langevin equation is formulated in terms of the particle velocity. In order to make connection with the time evolution of a real-space random walker, Eq. (3.33), we multiply the Langevin equation (3.43) by x and take the ensemble average:

$$\langle x\, \dot{v}\rangle = -\gamma \langle x\, v\rangle \,+\, \frac{1}{m} \langle x\, \xi\rangle \;. \tag{3.48}$$

We note that

$$x\, v = x\, \dot{x} = \frac{\mathrm{d}}{\mathrm{d}t} \frac{x^2}{2}, \qquad x\, \dot{v} = x\, \ddot{x} = \frac{\mathrm{d}^2}{\mathrm{d}t^2} \frac{x^2}{2} - \dot{x}^2$$

and

$$\langle x\xi\rangle \;=\; \left\langle \xi(t) \int_0^t v(t') dt' \right\rangle \;=\; \int_0^t dt' \int_0^{t'} dt'' \frac{e^{-\gamma(t'-t'')}}{m} \underbrace{\langle \xi(t)\xi(t'')\rangle}_{Q\delta(t-t'')} \;=\; 0 \;,$$

where we have used (3.44) in the limit of large times and that $t'' < t$. We then find for Eq. (3.48)

$$\frac{\mathrm{d}^2}{\mathrm{d}t^2}\frac{\langle x^2\rangle}{2} - \langle v^2\rangle \;=\; -\gamma\,\frac{\mathrm{d}}{\mathrm{d}t}\frac{\langle x^2\rangle}{2}$$

or

$$\frac{\mathrm{d}^2}{\mathrm{d}t^2}\langle x^2\rangle \,+\, \gamma\,\frac{\mathrm{d}}{\mathrm{d}t}\langle x^2\rangle \;=\; 2\langle v^2\rangle \;=\; \frac{Q}{\gamma m^2}\;, \qquad (3.49)$$

with the help of the long-time result Eq. (3.47) for $\langle v^2\rangle$. The solution of Eq. (3.49) is

$$\langle x^2\rangle \;=\; \left[\gamma t - 1 + e^{-\gamma t}\right]\,\frac{Q}{\gamma^3 m^2}\;. \qquad (3.50)$$

For long times we find

$$\lim_{t\to\infty}\langle x^2\rangle \;\simeq\; \frac{Q}{\gamma^2 m^2}\,t \;\equiv\; 2Dt, \qquad D = \frac{Q}{2\gamma^2 m^2} \qquad (3.51)$$

diffusive behavior, compare Eq. (3.33). This shows that diffusion is microscopically due to a stochastic process, since $D \propto Q$.

3.3 Noise-Controlled Dynamics

Stochastic Systems A set of first-order differential equations with a stochastic term is generally denoted a "stochastic system". The Langevin equation (3.43) discussed in Sect. 3.2.3 is a prominent example. The stochastic term corresponds quite generally to noise. Depending on the circumstances, noise might be very important for the long-term dynamical behavior. Some examples of this are as follows:

– Neural Networks: Networks of interacting neurons are responsible for the cognitive information processing in the brain. They must remain functional also in the presence of noise and need to be stable as stochastic systems. In this case the introduction of a noise term to the evolution equation should not change the dynamics qualitatively. This postulate should be valid for the vast majorities of biological networks.
– Diffusion: The Langevin equation reduces, in the absence of noise, to a damped motion without an external driving force, with $v = 0$ acting as a global attractor. The stochastic term is therefore essential in the long-time limit, leading to diffusive behavior.
– Stochastic Escape and Stochastic Resonance: A particle trapped in a local minimum may escape this minimum by a noise-induced diffusion process; a phenomenon called "stochastic escape". Stochastic escape in a driven

bistable system leads to an even more subtle consequence of noise-induced dynamics, the "stochastic resonance".

3.3.1 Stochastic Escape

Drift Velocity We generalize the Langevin equation (3.43) and consider an external potential $V(x)$,

$$m\,\dot{v} = -m\,\gamma\,v \;+\; F(x) \;+\; \xi(t), \qquad\qquad F(x) = -V'(x) = -\frac{\mathrm{d}}{\mathrm{d}x}V(x)\ , \tag{3.52}$$

where v, m are the velocity and the mass of the particle, $\langle\xi(t)\rangle = 0$ and $\langle\xi(t)\xi(t')\rangle = Q\delta(t-t')$. In the absence of damping ($\gamma = 0$) and noise ($Q = 0$), Eq. (3.52) reduces to Newton's law.

We consider for a moment a constant force $F(x) = F$ and the absence of noise, $\xi(t) \equiv 0$. The system then reaches an equilibrium for $t \to \infty$ when relaxation and force cancel each other:

$$m\,\dot{v}_D = -m\,\gamma\,v_D \;+\; F \equiv 0, \qquad\qquad v_D = \frac{F}{\gamma m}\ . \tag{3.53}$$

v_D is called the "drift velocity". A typical example is the motion of electrons in a metallic wire. An applied voltage, which leads an electric field along the wire, induces an electrical current (Ohm's law). This results in the drifting electrons being continuously accelerated by the electrical field, while bumping into lattice imperfections or colliding with the lattice vibrations, i.e. the phonons.

The Fokker–Planck Equation We consider now an ensemble of particles diffusing in an external potential, and denote with $P(x,t)$ the density of particles at location x and time t. Particle number conservation defines the particle current density $J(x,t)$ via the continuity equation

$$\frac{\partial P(x,t)}{\partial t} \;+\; \frac{\partial J(x,t)}{\partial x} = 0. \tag{3.54}$$

There are two contributions, J_D and J_ξ, to the total particle current density, $J = J_D + J_\xi$, induced by the diffusion and by the stochastic motion respectively. We derive these two contributions in two steps.

In a first step we consider with $Q = 0$ the absence of noise in Eq. (3.52). The particles then move uniformly with the drift velocity v_D in the stationary limit, and the current density is

$$J_D = v_D\,P(x,t)\ .$$

In a second step we set the force to zero, $F = 0$, and derive the contribution J_ξ of the noise term $\sim \xi(t)$ to the particle current density. For this purpose we rewrite the diffusion equation (3.31)

$$\frac{\partial P(x,t)}{\partial t} = D\,\frac{\partial^2 P(x,t)}{\partial x^2} \equiv -\frac{\partial J_\xi(x,t)}{\partial x} \qquad\qquad \frac{\partial P(x,t)}{\partial t} + \frac{\partial J_\xi(x,t)}{\partial x} = 0$$

as a continuity equation, which allows us to determine the functional form of J_ξ,

$$J_\xi = -D\frac{\partial P(x,t)}{\partial x} \ . \tag{3.55}$$

Using the relation $D = Q/(2\gamma^2 m^2)$, see Eq. (3.51), and including the drift term we find

$$J(x,t) = v_D\,P(x,t) \,-\, D\,\frac{\partial P(x,t)}{\partial x} = \frac{F}{\gamma m}\,P(x,t) \,-\, \frac{Q}{2\gamma^2 m^2}\,\frac{\partial P(x,t)}{\partial x} \tag{3.56}$$

for the total current density $J = J_D + J_\xi$. Using expression (3.56) for the total particle current density in (3.54) one obtains the "Fokker–Planck" or "Smoluchowski" equation

$$\frac{\partial P(x,t)}{\partial t} = -\frac{\partial v_D\,P(x,t)}{\partial x} \,+\, \frac{\partial^2 D\,P(x,t)}{\partial x^2} \tag{3.57}$$

for the density distribution $P(x,t)$, where the first term on the right-hand side of (3.57) corresponds to ballistic transport and the second term to diffusion.

The Harmonic Potential We consider the harmonic confining potential

$$V(x) = \frac{f}{2}\,x^2, \qquad\qquad F(x) = -f\,x\ ,$$

and a stationary density distribution,

$$\frac{\mathrm{d}P(x,t)}{\mathrm{d}t} = 0 \qquad \Longrightarrow \qquad \frac{\mathrm{d}J(x,t)}{\mathrm{d}x} = 0\ .$$

Expression (3.56) yields then the differential equation

$$\frac{\mathrm{d}}{\mathrm{d}x}\left[\frac{f\,x}{\gamma\,m} + \frac{Q}{2\gamma^2 m^2}\frac{\mathrm{d}}{\mathrm{d}x}\right]\,P(x) = 0 = \frac{\mathrm{d}}{\mathrm{d}x}\left[\beta f x + \frac{\mathrm{d}}{\mathrm{d}x}\right]\,P(x),$$

with $\beta = 2\gamma m/Q$ and where for the stationary distribution function $P(x) = \lim_{t\to\infty} P(x,t)$. The system is confined and the steady-state current vanishes consequently. We find

$$\boxed{P(x) = A\,e^{-\beta\frac{f}{2}x^2} = A\,e^{-\beta V(x)}} \qquad\qquad A = \sqrt{\frac{f\gamma m}{\pi Q}}, \tag{3.58}$$

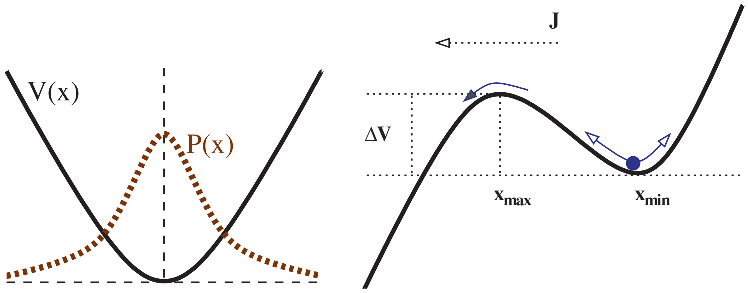

Fig. 3.12 *Left*: Stationary distribution $P(x)$ of diffusing particles in a harmonic potential $V(x)$. *Right*: Stochastic escape from a local minimum, with $\Delta V = V(x_{\mathrm{max}}) - V(x_{\mathrm{min}})$ being the potential barrier height and J the escape current

where the prefactor is determined by the normalization condition $\int \mathrm{d}x P(x) = 1$. The density of diffusing particles in a harmonic trap is Gaussian-distributed, see Fig. 3.12.

The Escape Current We now consider particles in a local minimum, as depicted in Fig. 3.12, with a typical potential having a functional form like

$$V(x) \;\sim\; -x + x^3 \;. \tag{3.59}$$

Without noise, the particle will oscillate around the local minimum eventually coming to a standstill $x \to x_{\mathrm{min}}$ under the influence of friction.

With noise, the particle will have a small but finite probability

$$\propto e^{-\beta \Delta V}, \qquad\qquad \Delta V = V(x_{\mathrm{max}}) - V(x_{\mathrm{min}})$$

to reach the next saddlepoint, where ΔV is the potential difference between the saddlepoint and the local minimum, see Fig. 3.12. The solution Eq. (3.58) for the stationary particle distribution in a confining potential $V(x)$ has a vanishing total current J. For non-confining potentials, like Eq. (3.59), the particle current $J(x,t)$ never vanishes. Stochastic escape occurs when starting with a density of diffusing particles close the local minimum, as illustrated in Fig. 3.12. The escape current will be nearly constant whenever the escape probability is small. In this case the escape current will be proportional to the probability a particle has to reach the saddlepoint,

$$J(x,t)\Big|_{x=x_{\mathrm{max}}} \;\propto\; e^{-\beta\,[V(x_{\mathrm{max}})-V(x_{\mathrm{min}})]} \;,$$

when approximating the functional dependence of $P(x)$ with that valid for the harmonic potential, Eq. (3.58).

Kramer's Escape When the escape current is finite, there is a finite probability per unit of time for the particle to escape the local minima, the *Kramer's escape rate* r_K,

$$r_K = \frac{\omega_{\max}\omega_{\min}}{2\pi\,\gamma}\;\exp\left[-\beta\left(V(x_{\max}) - V(x_{\min})\right)\right]\;, \tag{3.60}$$

where the prefactors $\omega_{\min} = \sqrt{|V''(x_{\min})|/m}$ and $\omega_{\max} = \sqrt{|V''(x_{\max})|/m}$ can be derived from a more detailed calculation, and where $\beta = 2\gamma m/Q$.

Stochastic Escape in Evolution Stochastic escape occurs in many real-world systems. Noise allows the system to escape from a local minimum where it would otherwise remain stuck for eternity.

As an example, we mention stochastic escape from a local fitness maximum (in evolution fitness is to be maximized) by random mutations that play the role of noise. These issues will be discussed in more detail in Chap. **??**.

3.3.2 Stochastic Resonance

The Driven Double-Well Potential We consider diffusive dynamics in a driven double-well potential, see Fig. 3.13,

$$\dot{x} = -V'(x) + A_0\cos(\Omega t) + \xi(t), \qquad V(x) = -\frac{1}{2}x^2 + \frac{1}{4}x^4\;. \tag{3.61}$$

The following is to be remarked:

– Equation (3.61) corresponds to the Langevin equation (3.52) in the limit of very large damping, $\gamma \gg m$, keeping $\gamma m \equiv 1$ constant (in dimensionless units).
– The potential in Eq. (3.61) is in normal form, which one can always achieve by rescaling the variables appropriately.
– The potential $V(x)$ has two minima x_0 at

$$-V'(x) = 0 = x - x^3 = x(1-x^2), \qquad x_0 = \pm 1\;.$$

  The local maximum $x_0 = 0$ is unstable.
– We assume that the periodic driving $\propto A_0$ is small enough, such that the effective potential $V(x) - A_0\cos(\Omega t)x$ retains two minima at all times, compare Fig. 3.13.

Transient State Dynamics The system will stay close to one of the two minima, $x \approx \pm 1$, for most of the time when both A_0 and the noise strength are weak, see Fig. 3.14. This is an instance of "transient state dynamics", which will be discussed in more detail in Chap. **??**. The system switches between a set of preferred states.

Switching Times An important question is then: How often does the system switch between the two preferred states $x \approx 1$ and $x \approx -1$? There are two time scales present:

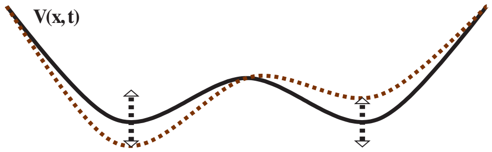

Fig. 3.13 The driven double-well potential, $V(x) - A_0\cos(\Omega t)x$, compare Eq. (3.61). The driving force is small enough to retain the two local minima

– In the absence of external driving, $A_0 \equiv 0$, the transitions are noise driven and irregular, with the average switching time given by Kramer's lifetime $T_K = 1/r_K$, see Fig. 3.14. The system is translational invariant with respect to time and the ensemble averaged expectation value

$$\langle x(t)\rangle \;=\; 0$$

therefore vanishes in the absence of an external force.
– When $A_0 \neq 0$ the external force induces a reference time and a non-zero response $\bar{x}$,

$$\langle x(t)\rangle = \bar{x}\,\cos(\Omega t - \bar{\phi})\ , \tag{3.62}$$

which follows the time evolution of the driving potential with a certain phase shift $\bar{\phi}$, see Fig. 3.15.

The Resonance Condition When the time scale $2T_K = 2/r_K$ to switch back and forth due to the stochastic process equals the period $2\pi/\Omega$, we expect a large response $\bar{x}$, see Fig. 3.15. The time-scale matching condition

$$\frac{2\pi}{\Omega} \;\approx\; \frac{2}{r_K}$$

depends on the noise-level Q, via Eq. (3.60), for the Kramer's escape rate r_K. The response $\bar{x}$ first increases with rising Q and then becomes smaller again, for otherwise constant parameters, see Fig. 3.15. Therefore the name "stochastic resonance".

Stochastic Resonance and the Ice Ages The average temperature T_e of the earth differs by about $\Delta T_e \approx 10\,^\circ\mathrm{C}$ in between a typical ice age and the interglacial periods. Both states of the climate are locally stable.

– The Ice Age: The large ice covering increases the albedo of the earth and a larger part of sunlight is reflected back to space. The earth remains cool.
– The Interglacial Period: The ice covering is small and a larger portion of the sunlight is absorbed by the oceans and land. The earth remains warm.

A parameter of the orbit of the planet earth, the eccentricity, varies slightly with a period $T = 2\pi/\Omega \approx 10^5$ years. The intensity of the incoming radiation from the sun therefore varies with the same period. Long-term climate changes can therefore be modeled by a driven two-state system, i.e. by

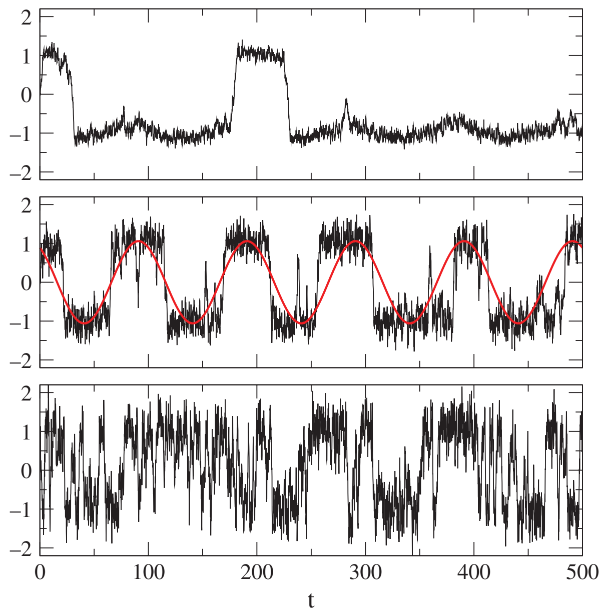

Fig. 3.14 Example trajectories $x(t)$ for the driven double-well potential. The strength and the period of the driving potential are $A_0 = 0.3$ and $2\pi/\Omega = 100$, respectively. The noise level Q is 0.05, 0.3 and 0.8 (*top*/*middle*/*bottom*), see Eq. (3.61)

Eq. (3.61). The driving force, viz the variation of the energy flux the earth receives from the sun, is however very small. The increase in the amount of incident sunlight is too weak to pull the earth out of an ice age into an interglacial period or vice versa. Random climatic fluctuation, like variations in the strength of the gulf stream, are needed to finish the job. The alternation of ice ages with interglacial periods may therefore be modeled as a stochastic resonance phenomenon.

Neural Networks and Stochastic Resonance Neurons are driven bistable devices operating in a noisy environment. It is therefore not surprising that stochastic resonance may play a role for certain neural network setups with undercritical driving.

Beyond Stochastic Resonance Resonance phenomena generally occur when two frequencies, or two time scales, match as a function of some control parameter. For the case of stochastic resonance these two time scales correspond to the period of the external driving and to the average waiting time for the Kramer's escape respectively, with the later depending directly on the level of the noise. The phenomenon is denoted as "stochastic resonance" since one of the time scales involved is controlled by the noise.

One generalization of this concept is the one of "coherence resonance". In this case one has a dynamical system with two internal time scales t_1 and

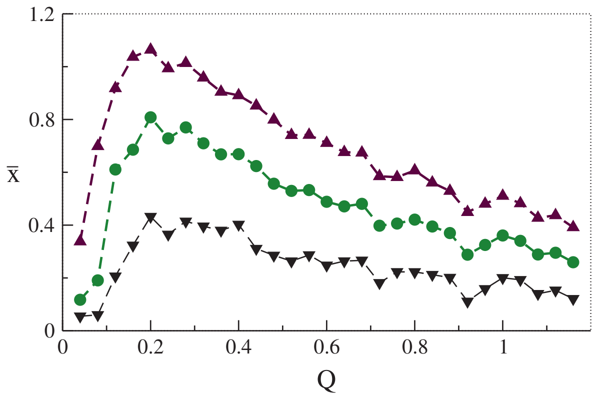

Fig. 3.15 The gain $\bar{x}$, see Eq. (3.62), as a function of noise level Q. The strength of the driving amplitude A_0 is 0.1, 0.2 and 0.3 (*bottom/middle/top curves*), see Eq. (3.61) and the period $2\pi/\Omega = 100$. The response $\bar{x}$ is very small for vanishing noise $Q = 0$, when the system performs only small-amplitude oscillations in one of the local minima

t_2. These two time scales will generally be affected to a different degree by an additional source of noise. The stochastic term may therefore change the ratio t_1/t_2, leading to internal resonance phenomena.

Exercises

The logistic map and the shift map

With the representation $x_n = (1 - \cos(\pi\theta_n))/2$ show that the logistic map (**??**) is equivalent, for $r = 4$, to the shift map

$$\theta_{n+1} = (2\theta_n)\%1 = \begin{cases} 2\theta_n & \text{for} \quad 0 < \theta < 0.5 \\ 2\theta_n - 1 & \text{for } 0.5 < \theta < 1 \end{cases} \tag{3.63}$$

where the %-sign denotes the modulus operation. This representation can be used to evaluate analytically the distribution $p(x)$ of finding x when iterating the logistic map ad infinitum.

Fixpoints of the Lorenz Model

Perform the stability analysis of the fixpoint $(0,0,0)$ and of $C_{+,-} = (\pm\sqrt{b(r-1)}, \pm\sqrt{b(r-1)}, r-1)$ for the Lorenz model Eq. (3.7) with $r, b > 0$. Discuss the difference between the dissipative case and the ergodic case $\sigma = -1 - b$, see Eq. (3.9).

The Hausdorff Dimension

Calculate the Hausdorff dimension of a straight line and of the Cantor set, which is generated by removing consecutively the middle-1/3 segment of a line having a given initial length.

The Driven Harmonic Oscillator

Solve the driven, damped harmonic oscillator

$$\ddot{x} + \gamma\,\dot{x} + \omega_0^2\,x = \epsilon\cos(\omega t)$$

in the long-time limit. Discuss the behavior close to the resonance $\omega \to \omega_0$.

Markov Chain of Umbrellas

Lady Ann has four umbrellas which she uses whenever it rains to go from work to home, or vice versa. She takes only an umbrella with her whenever it rains, leaving the umbrellas otherwise in the office and at home respectively. It rains with probability $p \in [0,1]$. How often does Lady Ann get wet?

Biased Random Walk

Generalize the derivation of the diffusion equation (3.31) for a random walker jumping with probabilities $(1 \pm \alpha)/2$ either to the right or to the left, with $\alpha \in [-1:1]$. How does α needs to scale such that a non-trivial contribution is retained in the limit $\Delta t \to 0$ and $\Delta x \to 0$? What kind of solutions does one find for a vanishing diffusion constant $D \to 0$?

Continuous-Time Logistic Equation

Consider the continuous-time logistic equation

$$\dot{y}(t) = \alpha y(t)\Big[1 - y(t)\Big]\ .$$

(A) Find the general solution and (B) compare to the logistic map Eq. (**??**) for discrete times $t = 0,\ \Delta t,\ 2\Delta t,\ ...$

Further Reading

For further studies we refer to introductory texts for dynamical system theory Katok (1995), classical dynamical systems Goldstein (2002), chaos Schuster (2005); Devaney (1989); Gutzwiller (1990); Strogatz (1994), stochastic systems Ross (1982); Lasota (1994) and differential equations with time delays Erneux (2009). Other textbooks on complex and/or adaptive systems are those by Schuster (2001) and Boccara (2003). For an alternative approach to complex system theory via Brownian agents consult Schweitzer (2003).

The interested reader may want to study some selected subjects in more depth, such as the KAM theorem Ott (2002), relaxation oscillators Wang (1999), stochastic resonance Benzit et al. (1981); Gammaitoni et al. (1998), coherence resonance Pikovsky (1997), Lévy flights Metzler (2000), the connection of Lévy flights to the patterns of wandering albatrosses Viswanathan et al. (1996), human traveling Brockmann et al. (2006) and diffusion of information in networks Eriksen et al. (2003).

The original literature provides more insight, such as the seminal works of Einstein (1905) and Langevin (1908) on Brownian motion or the first formulation and study of the Lorenz (1963) model.

References

Benzit, R., Sutera, A., Vulpiani, A. 1981 The mechanism of stochastic resonance. *Journal of Physics A* **14**, L453–L457.

Boccara, N. 2003 *Modeling Complex Systems.* Springer, Berlin.

Brockmann, D., Hufnagel, L., Geisel, T. 2006 The scaling laws of human travel. *Nature* **439**, 462.

Devaney, R.L. 1989 *An Introduction to Chaotic Dynamical Systems.* Addison-Wesley, Reading, MA.

Einstein, A. 1905 Über die von der molekularkinetischen Theorie der Wärme geforderte Bewegung von in ruhenden Flüssigkeiten suspendierten Teilchen. *Annalen der Physik* **17**, 549.

Eriksen, K.A., Simonsen, I., Maslov, S., Sneppen, K. 2003 Modularity and extreme edges of the internet. *Physical Review Letters* **90**, 148701.

Erneux, T. 2009 *Applied Delay Differential Equations.* Springer, New York.

Gammaitoni, L., Hänggi, P., Jung, P., Marchesoni, F. 1998 Stochastic resonance. *Review of Modern Physics* **70**, 223–287.

Goldstein, H. 2002 *Classical Mechanics.* 3rd Edition, Addison-Wesley, Reading, MA.

Gutzwiller, M.C. 1990 *Chaos in Classical and Quantum Mechanics.* Springer, New York.

Katok, A., Hasselblatt, B. 1995 *Introduction to the Modern Theory of Dynamical Systems.* Cambridge University Press, Cambridge.

Langevin, P. 1908 Sur la théorie du mouvement brownien. *Comptes Rendus* **146**, 530–532.

Lasota, A., Mackey, M.C. 1994 *Chaos, Fractals, and Noise – Stochastic Aspects of Dynamics.* Springer, New York.

Lorenz, E.N. 1963 Deterministic nonperiodic flow. *Journal of the Atmospheric Sciences* **20**, 130–141.

Metzler, R., Klafter J. 2000 The random walk's guide to anomalous diffusion: A fractional dynamics approach. *Physics Reports* **339**, 1.

Ott, E. 2002 *Chaos in Dynamical Systems.* Cambridge University Press, Cambridge.

Pikovsky, A.S., Kurths, J. 1997 Coherence resonance in a noise-driven excitable system. *Physical Review Letters* **78**, 775.

Ross, S.M. 1982 *Stochastic Processes.* Wiley, New York.

Schuster, H.G. 2001 *Complex Adaptive Systems.* Scator, Saarbrücken.

Schuster, H.G., Just, W. 2005 *Deterministic Chaos.* 4th Edition, Wiley-VCH, New York.

Schweitzer, F. 2003 *Brownian Agents and Active Particles: Collective Dynamics in the Natural and Social Sciences.* Springer, New York.

Strogatz, S.H. 1994 *Nonlinear Systems and Chaos.* Perseus Publishing, Cambridge, MA.

Viswanathan, G.M., Afanasyev, V., Buldyrev, S.V., Murphy, E.J., Prince, P.A., Stanley, H.E. 1996 Lévy flight search patterns of wandering albatrosses. *Nature* **381**, 413.

Wang, D.L. 1999 *Relaxation oscillators and networks* In Webster, J.G. (ed.), *Encyclopedia of Electrical and Electronic Engineers*, pp. 396–405. Wiley, New York.